Molecular Cell, Vol. 10, 549–561, September, 2002, Copyright ©2002 by Cell Press

RNAi in Human Cells: Basic Structural and Functional Features of Small Interfering RNA

Ya-Lin Chiu and Tariq M. Rana[1]
Chemical Biology Program
Department of Biochemistry
and Molecular Pharmacology
University of Massachusetts Medical School
364 Plantation Street
Worcester, Massachusetts 01605

Summary

We investigated the mechanism of RNA interference (RNAi) in human cells. Here we demonstrate that the status of the 5′ hydroxyl terminus of the antisense strand of a siRNA determines RNAi activity, while a 3′ terminus block is tolerated in vivo. 5′ hydroxyl termini of antisense strands isolated from human cells were phosphorylated, and 3′ end biotin groups were not efficiently removed. We found no requirement for a perfect A-form helix in siRNA for interference effects, but an A-form structure was required for antisense-target RNA duplexes. Strikingly, crosslinking of the siRNA duplex by psoralen did not completely block RNA interference, indicating that complete unwinding of the siRNA helix is not necessary for RNAi activity in vivo. These results suggest that RNA amplification by RNA-dependent RNA polymerase is not essential for RNAi in human cells.

Introduction

RNAi interference (RNAi) is the process whereby double-stranded RNA (dsRNA) induces the sequence-specific degradation of homologous mRNA. Although RNAi was first discovered in *Caenorhabditis elegans* (Fire et al., 1998), similar phenomena had been reported in plants (posttranscriptional gene silencing [PTGS]) and in *Neurospora crassa* (quelling) (reviewed in Hammond et al., 2001; Sharp, 2001). It has become clear that dsRNA-induced silencing phenomena are present in evolutionarily diverse organisms, e.g., nematodes, plants, fungi, and trypanosomes (Bass, 2000; Cogoni and Macino, 2000; Fire et al., 1998; Hammond et al., 2001; Ketting and Plasterk, 2000; Matzke et al., 2001; Sharp, 2001; Sijen and Kooter, 2000; Tuschl, 2001; Waterhouse et al., 2001). Biochemical studies in *Drosophila* embryo lysates and S2 cell extracts have begun to unravel the mechanisms by which RNAi works (Bernstein et al., 2001; Tuschl et al., 1999; Zamore et al., 2000).

RNAi is initiated by an ATP-dependent, processive cleavage of dsRNA into 21 to 23 nucleotide (nt) short interfering RNAs (siRNAs) (Bernstein et al., 2001; Hamilton and Baulcombe, 1999; Hammond et al., 2000; Zamore et al., 2000) by the enzyme Dicer, a member of the RNase III family of dsRNA-specific endonucleases (Bernstein et al., 2001). These native siRNA duplexes containing 5′ phosphate and 3′ hydroxyl termini are then incorporated into a protein complex called RNA-induced silencing complex (RISC) (Hammond et al., 2000). ATP-dependent unwinding of the siRNA duplex generates an active complex, RISC* (the asterisk indicates the active conformation of the complex) (Nykanen et al., 2001). Guided by the antisense strand of siRNA, RISC* recognizes and cleaves the corresponding mRNA (Elbashir et al., 2001b; Hammond et al., 2000; Nykanen et al., 2001).

Recently, Tuschl and colleagues (Elbashir et al., 2001a) have demonstrated that RNAi can be induced in numerous mammalian cell lines by introducing synthetic 21 nt siRNAs. By virtue of their small size, these siRNAs avoid provoking an interferon response that activates the protein kinase PKR (Stark et al., 1998). Functional anatomy studies of synthetic siRNA in *Drosophila* cell lysates have demonstrated that each siRNA duplex cleaves its target RNA at a single site (Elbashir et al., 2001c). The 5′ end of the guide siRNA sets the ruler for defining the position of target RNA cleavage (Elbashir et al., 2001c). 5′ phosphorylation of the antisense strand is required for effective RNA interference in vitro (Nykanen et al., 2001). Mutation studies have shown that a single mutation within the center of a siRNA duplex discriminates between mismatched targets (Elbashir et al., 2001c). These experiments showed a more stringent requirement for the antisense strand of the trigger dsRNA as compared to the sense strand (Grishok et al., 2000; Parrish et al., 2000). However, none of these phenomena have been demonstrated in vivo, especially in mammalian systems.

A particularly fascinating aspect of RNAi is its extraordinary efficiency. It has been estimated that in *Drosophila* embryos, ~35 molecules of dsRNA can silence a target mRNA thought to be present at >1000 copies per cell (Kennerdell and Carthew, 1998). Conversion of the long trigger dsRNA into many 21 to 23 nt siRNA fragments would, itself, provide some degree of amplification. Another plausible explanation for the potency of interference is that the RISC* is a multiple-turnover enzyme, which can catalytically perform the targeting and cleavage activity. The involvement of RNA-dependent RNA polymerase (RdRP) in the amplification process has recently been postulated since genetic screening has identified the gene for RdRP as a requirement for gene silencing in plants, fungi, and worms (Cogoni and Macino, 1999; Dalmay et al., 2000; Mourrain et al., 2000; Sijen et al., 2001). A random degradative PCR model has been suggested (Lipardi et al., 2001; Nishikura, 2001; Sijen et al., 2001), in which siRNA serves as the primer for the RdRP reaction. The siRNA-primed RdRP converts target mRNA into dsRNA, which can serve as Dicer substrates, initiating the RdRP chain reaction. The polarity of the RdRP reaction limits the synthesis of secondary siRNAs to the region upstream of the trigger sequence. Certain structural features of siRNA, including the 3′ hydroxyl group and 5′ phosphate group, are critical for the RdRP reaction and RNA ligation (Lipardi et al., 2001; Sijen et al., 2001). A number of apparent constraints on the role of RdRP activity in RNAi, however, severely limit models in which RdRP carries out

[1]Correspondence: tariq.rana@umassmed.edu

a multiround replication of a double-stranded trigger. Experiments using siRNA with two differentially modified strands (Parrish et al., 2000; Yang et al., 2000) have shown a more stringent requirement for the antisense strand of the original trigger as compared to the sense strand. Multiround replication of a double-stranded trigger by RdRP would result in loss of memory of the difference between the original two strands and thus be incompatible with the observed effects of strand-specific modification. Although RdRP activity has been reported in *Drosophila* embryo lysates (Lipardi et al., 2001), a homolog of RdRP has not been identified in available mammalian genomic sequences.

A number of basic questions remain to be answered regarding RNA interference in human cells. (1) What is the kinetics of RNAi? (2) Is 5′ OH required for kinase activity and is it phosphorylated in vivo? (3) Is 3′ OH required for RNA-dependent RNA polymerase-like activity? (4) Is an A-form helix of dsRNA required for RNAi? If yes, at which stage during the pathway? (5) Is complete unwinding of the dsRNA helix necessary to cause RNAi effects? This article addresses these issues.

Results

Dual Fluorescence Reporter System for RNAi Analysis in Mammalian Cells

To explore the functional anatomy of siRNA in mammalian cells, we established a dual fluorescence reporter system, using HeLa cells as a model system. Two reporter plasmids were used: pEGFP-C1 and pDsRed1-N1, harboring enhanced green fluorescent protein (GFP) or coral (*Discosoma spp*.)-derived red fluorescent protein (RFP), respectively. The expression of these reporter genes was under cytomegalovirus promoter control and could be easily visualized by fluorescence microscopy in living cells. The siRNA sequence targeting GFP was from position 238–258 relative to the start codon, and the RFP siRNA sequence was from position 277–297 relative to the start codon (Figure 1A). Using lipofectamine, we cotransfected HeLa cells with pEGFP-C1 and pDsRed1-N1 expression plasmids and siRNA duplex, targeting either GFP or RFP. Fluorescence imaging was used to monitor GFP and RFP expression levels. As shown in Figures 1Ba and 1Bb, mock treatment (without siRNA) allowed efficient expression of both GFP and RFP in living cells. Transfection of cells with siRNA duplex targeting GFP (GFP ds) significantly reduced GFP expression (Figure 1Bc) but had no effect on RFP expression (Figure 1Bd) compared with mock-treated cells (Figures 1Ba and 1Bb). On the other hand, transfection of cells with siRNA duplex targeted to RFP (RFP ds) significantly interfered with the expression of RFP but not GFP (Figures 1Be and 1Bf).

To quantify RNAi effects, we prepared lysates from siRNA duplex-treated cells at 42 hr posttransfection. GFP and RFP fluorescence in clear lysates was measured on a fluorescence spectrophotometer. The peak at 507 nm (Figure 1C, left panel) represents the fluorescence intensity of GFP, and the peak at 583 nm (Figure 1C, right panel) represents the fluorescence intensity of RFP. GFP fluorescence intensity of GFP ds-treated cells (Figure 1C, left panel, green line) was only 5% of mock-treated (black line) or RFP ds-treated cells (cyan line). In contrast to GFP fluorescence, RFP fluorescence intensity (Figure 1C, right panel) significantly decreased only in cells treated with RFP ds (red line), indicating the specificity of the RNAi effect.

To confirm these findings on RNAi effects in living mammalian cells, we carried out Western blotting experiments (Supplemental Figure S1 at http://www.molecule.org/cgi/content/full/10/3/549/DC1) using anti-GFP and anti-RFP antibodies. Analysis of immunoblots revealed that the siRNA targeting GFP inhibited only GFP expression without affecting RFP levels (Supplemental Figure S1A at http://www.molecule.org/cgi/content/full/10/3/549/DC1, lanes 9–14); siRNA targeting RFP was similarly specific against RFP expression (Supplemental Figure S1B at http://www.molecule.org/cgi/content/full/10/3/549/DC1, lanes 9–14). This RNA interference effect depended on the presence of 21 nucleotide duplex siRNA but not of the antisense strand siRNA (Supplemental Figures S1A and S1B at http://www.molecule.org/cgi/content/full/10/3/549/DC1, compare right and left panels). These results demonstrate that we have established a reliable and quantitative system for studying specific RNA interference in HeLa cells.

Kinetics of RNA Interference in HeLa Cells

One of the many intriguing features of gene silencing by RNA interference is its unusually high efficiency—a few dsRNA molecules suffice to inactivate a continuously transcribed target mRNA for long periods of time. It has been demonstrated in plants (Cogoni and Macino, 1999; Dalmay et al., 2000) and worms (Grishok et al., 2000) that this inactivation can spread throughout the organism and is often heritable to the next generation. Mutations in genes encoding a protein related to RdRP affect RNAi-type processes in *Neurospora* (QDE-1; Cogoni and Macino, 1999), *C. elegans* (EGO-1; Smardon et al., 2000), and plants ([SGS2; Mourrain et al., 2000] and [SDE-1; Dalmay et al., 2000]). The involvement of RdRP in amplifying RNAi has been postulated (Lipardi et al., 2001).

To understand the kinetics of gene suppression and persistence of RNA interference in HeLa cells, we prepared lysates from cells cotransfected with GFP siRNA and dual fluorescence reporter plasmids, pEGFP-C1 and pDsRed1-N1. In this experiment, GFP was the target of the duplex siRNA, while RFP was used as a control for transfection efficiency and specificity of RNA interference. Emission spectra of GFP in cell lysates at various times after transfection (Supplemental Figure S2 at http://www.molecule.org/cgi/content/full/10/3/549/DC1) show that siRNA duplex caused an RNA interference effect as early as 6 hr posttransfection. This effect gradually increased with time, peaking at 42 hr, then started to decrease at 66 hr (Supplemental Figure S2 at http://www.molecule.org/cgi/content/full/10/3/549/DC1, green lines). As a control experiment, GFP expression in the presence of antisense strand was also monitored and showed no RNAi effects (Supplemental Figure S2 at http://www.molecule.org/cgi/content/full/10/3/549/DC1, blue lines). Thus, RNA interference can last for at least 66 hr in HeLa cells (Supplemental Figure S2 at http://www.molecule.org/cgi/content/full/10/3/549/DC1, green lines).

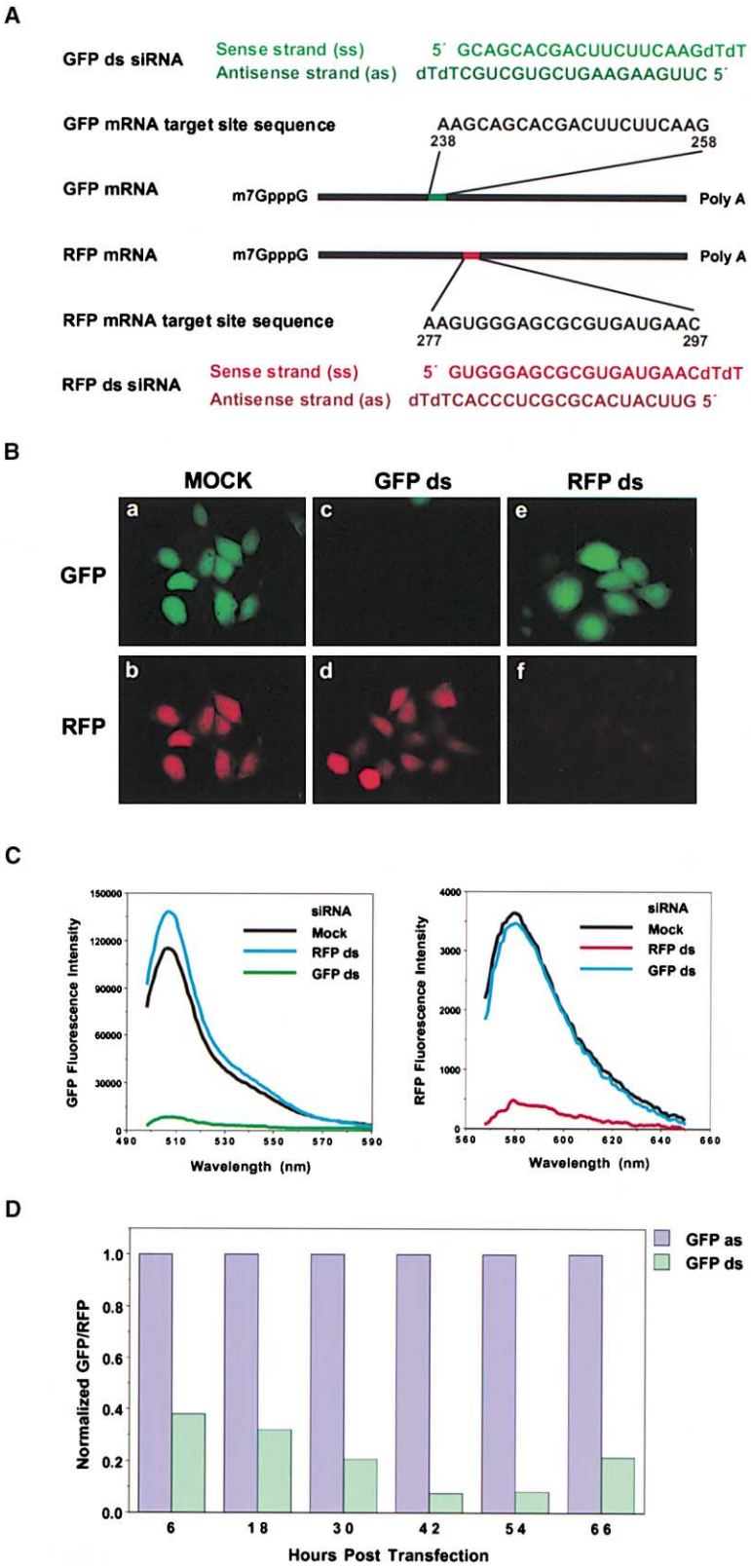

Figure 1. Dual Fluorescence Reporter Assay System for RNAi Analysis in HeLa Cells

(A) Graphical representation of dsRNAs used for targeting GFP mRNA and RFP mRNA. GFP and RFP were encoded by the pEGFP-C1 and pDsRed1-N1 reporter plasmid, respectively. siRNAs were synthesized with 2 nt deoxythymidine overhangs at the 3′ end. The position of the first nucleotide of the mRNA target site is indicated relative to the start codon of GFP mRNA or RFP mRNA. The sequence of the antisense strand of siRNA is exactly complementary to the mRNA target site.

(B) Fluorescence images showing specific RNA interference effects in living HeLa cells. Fluorescence in living cells was visualized by fluorescence microscopy at 48 hr posttransfection. (a) and (b), images of mock-treated cells (no siRNA added); (c) and (d), images of GFP siRNA-treated cells; (e) and (f), images of RFP siRNA-treated cells.

(C) Quantitative analysis of RNAi effects in HeLa cells. Fluorescence emission spectra of GFP and RFP in total cell lysates were detected by exciting at 488 and 568 nm, respectively.

(D) Kinetics of RNAi effects in HeLa cells. Ratios of normalized GFP to RFP fluorescence intensity over a 66 hr time course. The fluorescence intensity ratio of target (GFP) to control (RFP) protein was determined in the presence of double-strand (ds) RNA (green bars) and normalized to the ratio observed in the presence of antisense strand (as) RNA (blue bars). Normalized ratios less than 1.0 indicate specific RNA interference. Maximal RNAi effect occurred at 42 hr posttransfection.

To quantify the kinetics of RNA interference, we measured the fluorescence intensity ratio of target (GFP) to control (RFP) fluorophore in the presence of siRNA duplex (ds) and normalized it to the ratio observed in the presence of antisense strand siRNA (as). Normalized ratios less than 1.0 indicate specific interference. As shown in Figure 1D, at 6 hr posttransfection GFP duplex siRNA (green bars) inhibits 60% of GFP expression com-

pared to antisense strand siRNA (blue bars). RNA interference reached its maximum (92% inhibition) at 42 hr posttransfection; only 8% of normal GFP expression was observed in duplex siRNA-treated cells. These results show that RNA interference can suppress target protein expression up to 66 hr, although maximum activities were observed at 42–54 hr posttransfection.

Free 5′ OH Groups on the Antisense Strand of the siRNA Duplex Are Required for RNA Interference In Vivo

Synthetic 21 nucleotide siRNA duplexes with 5′ hydroxyl termini and 3′ overhang have been shown to specifically suppress expression of endogenous and heterologous genes in *Drosophila* extracts (Elbashir et al., 2001b) and mammalian cell lines (Elbashir et al., 2001a). Nonetheless, native siRNA, processed by Dicer cleavage of dsRNA, contains 5′ phosphate ends (Elbashir et al., 2001b). It has been demonstrated in vitro that *Drosophila* embryo lysates contain a potent kinase activity that phosphorylates the 5′ hydroxyl termini of synthetic siRNAs (Nykanen et al., 2001). The 5′ phosphate is required on the siRNA strand that guides target cleavage in RNA interference (Nykanen et al., 2001).

To examine the importance of 5′ termini of siRNA in RNA interference in human cells, we modified synthetic siRNAs targeting GFP by using an amino group with a 3-carbon linker (5′ N3, Figure 2A) to block their 5′ termini. Synthetic siRNAs with this modification lacked a hydroxyl group to be phosphorylated by kinases in vivo. This modification could also block access to siRNA by cellular factors that might require recognizing the 5′ OH termini. We annealed unmodified siRNA strands with 5′ modified strands, producing siRNA duplexes with 5′ modification at only the sense strand (5′-N3ss/as), at only the antisense strand (ss/5′-N3as), or at both strands (5′-N3ss/5′-N3as) (Figure 2B). RNAi effects of these siRNA duplexes were analyzed in our dual fluorescence reporter system as described in Figure 1. 5′ modification of the sense strand had no effect on RNAi activity (Figures 3b and 3c), whereas 5′ modification of the antisense strand completely abolished the RNAi effect (Figures 3d and 3e; Figures 4A and 4B, upper panels). HeLa cells transfected with antisense strand (as) siRNA as control showed no RNAi activity (Figure 3a). These results demonstrate that the 5′ OH in the antisense strand of the siRNA duplex is an important determinant of RNAi activity in human cells.

Blocking the 3′ End of siRNAs Has Little Effect on RNA Interference In Vivo

To determine the effect of 3′ OH groups on RNAi activity, we synthesized siRNA duplexes containing a 3′ end blocked with 3′ puromycin (3′-Pmn, Figure 2A) or biotin instead of 3′ OH groups on the overhang deoxythymidine (Figure 2B). These 3′ end modifications would block any processing of the siRNA duplex that required a free 3′ hydroxyl group. We prepared three combinations of siRNA duplexes containing 3′ puromycin: 3′ blocked at only the sense strand (ss3′-Pmn/as), at only the antisense strand (ss/as3′-Pmn), or at both strands (ss3′-Pmn/as3′-Pmn) (Figure 2B). We also prepared a siRNA duplex containing biotin at the 3′ end of antisense strand (ss/as3′-Biotin). The RNAi activities of these siRNA duplexes were analyzed in our dual fluorescence reporter system. Results of these experiments indicate that a 3′ block at either the sense or antisense strand of siRNA duplex had little effect on its RNA interference activity (Figures 3f–3i; Figures 4A and 4B, middle panels). Furthermore, biotin pull-out experiments showed that the 3′ end biotin groups on the antisense strand were not efficiently removed during RNAi activities in HeLa cells (Figure 5, see below). Modifications could be introduced in the 3′ overhangs without affecting siRNA efficacy, suggesting that RNA interference in mammalian cells does not occur through the recently reported RdRP-dependent degradative PCR mechanism (Lipardi et al., 2001; Sijen et al., 2001), which requires a free 3′ hydroxyl group.

A-Form Helix of siRNA Is Absolutely Required for Effective RNA Interference In Vivo

Synthetic and native siRNAs, generated from ATP-dependent cleavage of double-strand RNA, have been proposed to act as "guide RNAs" that target an associated nuclease complex, the RISC (RNA-induced silencing complex), to the corresponding mRNA through strand complementarity (Hammond et al., 2000; Nykanen et al., 2001). How are these siRNA duplexes recognized and incorporated into the RISC protein complex? siRNA duplexes are readily characterized by their A-form helix, which can be distinguished from the structures of B-form helix DNA and single-stranded RNA in the cell. A single mismatch between a target mRNA and its guide strand siRNA completely prevents target RNA cleavage in *Drosophila* embryo lysates (Elbashir et al., 2001c). Although the mechanism of target recognition has not been experimentally demonstrated, this finding indicates that recognition requires exact complementarity between the guide strand and target mRNA.

These observations raise two fundamental questions regarding RNAi effects in vivo. (1) Is an A-form RNA helix required in the siRNA structure? (2) Is an A-form helix recognized by proteins after the antisense strand of siRNA duplex is hybridized with the target mRNA? To address these questions, we designed three siRNA duplexes containing internal bulge structures in the RNA helices (Figure 2B). The A-form RNA helix has a deep, narrow major groove and a shallow, wide minor groove. More than one nucleotide bulge has been shown to distort RNA helical structures, widening the major groove and enhancing accessibility to its functional groups (Neenhold and Rana, 1995; Weeks and Crothers, 1991, 1993). We decided to use 2 nt bulges to generate distorted A-form helices in siRNAs. We synthesized mutant siRNA by introducing two extra nucleotides into the sense or antisense strand of siRNA duplexes. Combining these mutant siRNA strands with original siRNA sequences produced three siRNA duplexes with an internal bulge at only the sense strand (ss-bulge/as), at only the antisense strand (ss/as-bulge), or at both strands (ss-bulge/as-bulge) (Figure 2B). This design of bulge-containing siRNAs could dissect the requirement for the A-form helix at two different steps of RNA interference: (1) siRNA recognition by RISC and (2) RISC targeting of mRNA via the guiding siRNA. siRNA duplexes with an

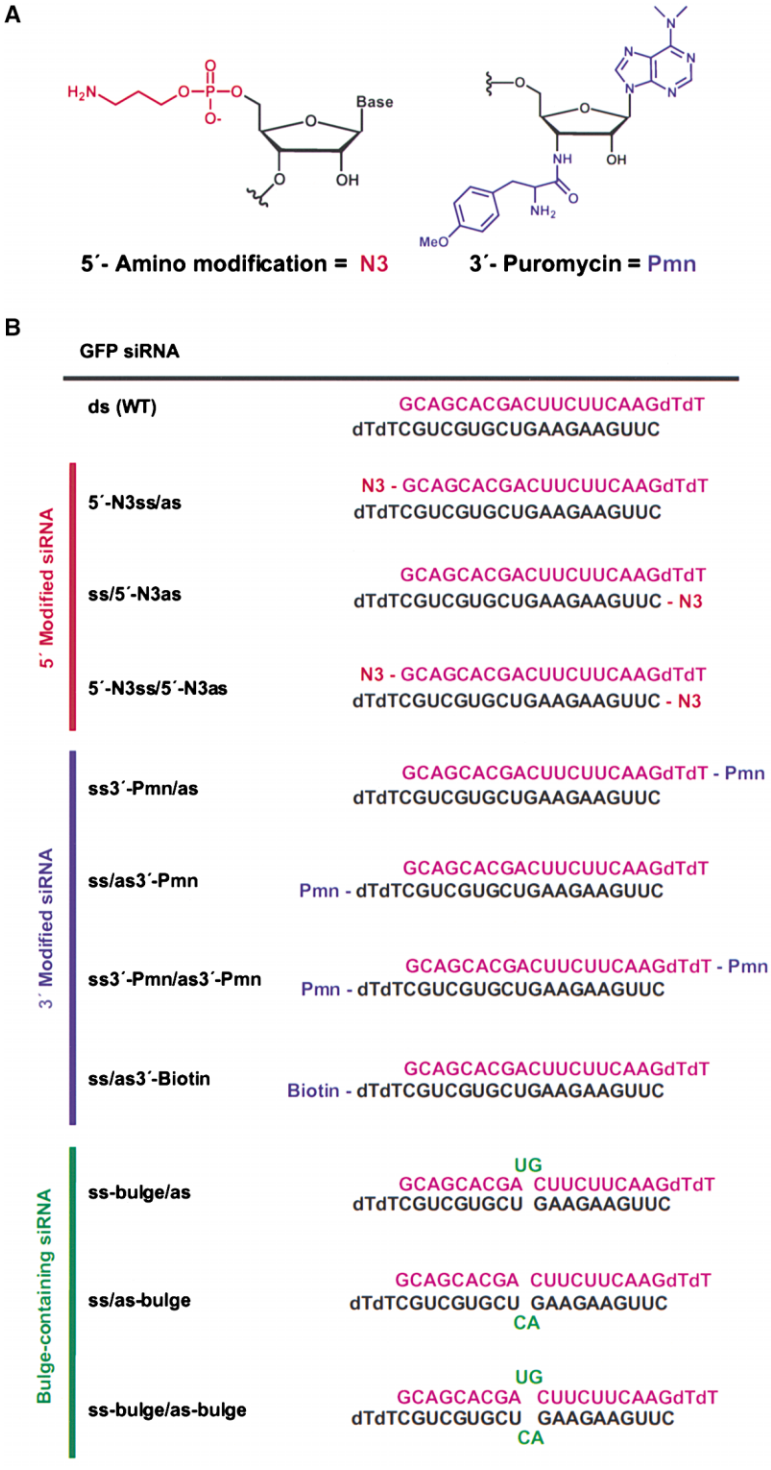

Figure 2. Modification of GFP siRNA Duplexes

(A) Structure of 5′-N3 (amino group with 3-carbon linker, red) and 3′-Pmn (puromycin, blue) modifications.

(B) Classification and nomenclature of the modified siRNAs. Sense (top row, purple) and antisense (bottom row, black) strands of siRNA species are shown with their 5′-N3 (red) and 3′-Pmn or biotin (blue) modifications. A dinucleotide internal bulge structure (green) was introduced in sense, antisense, or duplex RNAs.

internal bulge at only the sense strand (ss-bulge/as) caused a structural change in the siRNA duplex (an imperfect A-form) without affecting the complementarity between target mRNA and the antisense strand, which acts as the guiding strand in the RNA interference pathway. RNA interference by these siRNA duplexes was analyzed and quantified in our dual fluorescence reporter system as described above.

Surprisingly, the siRNA duplex containing a bulge in its sense strand retained most of its RNA interference activity (compare Figures 3b and 3j; Figures 4A and 4B, lower panels, green line and bars), indicating that an A-form siRNA helix is not essential for effective RNA interference in vivo. However, bulges in the antisense strand or both strands of duplex siRNA completely abolished RNA interference ability (Figures 3k and 3l; Figures 4A and 4B, lower panels, dark and light blue line and bars), indicating that effective RNA interference in vivo

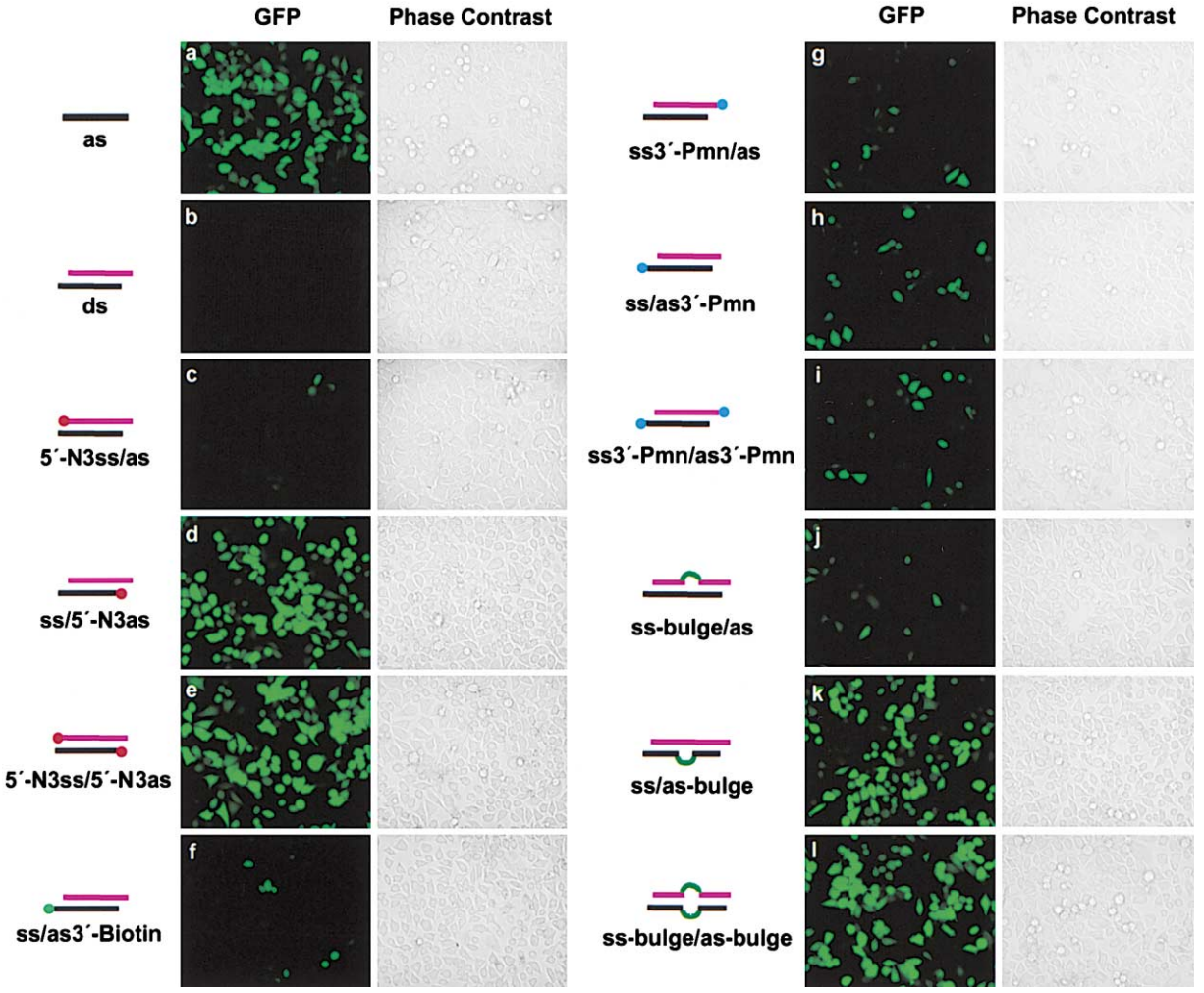

Figure 3. Fluorescence Images Showing RNA Interference Effects in Living HeLa Cells Transfected with Modified siRNA Duplexes

HeLa cells were cotransfected by lipofectamine with pEGFP-C1, pDsRed1-N1 reporter plasmids and siRNA with a 5′ modification (c–e), 3′ modification (f–i), or internal bulge (j–l). Fluorescence in living cells was visualized at 48 hr posttransfection. GFP fluorescence (left panels) and phase contrast images (right panels) are shown. RNA used in each experiment is indicated on the left of each pair of panels.

absolutely requires A-form helix formation between target mRNA and its guiding antisense strand.

5′ OH Groups on the Antisense Strand of the siRNA Duplex Are Phosphorylated In Vivo

To analyze the phosphorylation status of the 5′ termini of siRNA and to probe the participation of siRNA 3′ termini in the RNA interference pathway in vivo, we transfected HeLa cells with 21 nt RNAs containing biotin at the 3′ terminal of the antisense strand (ss/as3′-Biotin) and isolated the biotinylated siRNA at various times after transfection (see Experimental Procedures). In brief, streptavidin magnetic beads were used to pull out biotinylated siRNAs from transfected cells, washed to remove unbound RNA, and split into two aliquots. One aliquot was dephosphorylated with shrimp alkaline phosphatase (SAP), and the RNA 5′ ends were labeled with ^{32}P by T4 polynucleotide kinase (PNK) reaction. The other aliquot was subjected to 5′ end radiolabeling with polynucleotide kinase without prior dephosphorylation reaction with SAP. RNA was resolved on 20% polyacrylamide-7 M urea gels and visualized by phosphorimager analysis. Cells without siRNA treatment showed no detectable signal after biotin pull-out assay (Figure 5, lane 4), indicating the absence of nonspecific RNA-bead interactions. Efficient 5′ end radiolabeling was observed only when RNA was pretreated with phosphatase (compare lanes 5–9 and 10–14), indicating that the 5′ termini of siRNA did not contain free OH groups in vivo. Although phosphorylating with SAP and quenching the phosphatase reaction by heating resulted in some RNA degradation, the efficiency of the kinase reaction after SAP treatment is obvious. These results indicate that 5′ OH groups are phosphorylated in vivo for RNAi activities.

These experiments demonstrate three key findings. First, biotinylated-siRNA can be isolated from HeLa cells at 6 to 54 hr posttransfection (Figure 5, lanes 5–9). The amount of isolated siRNA decreased in a time-dependent manner, indicating the degradation of siRNA in vivo. Our dual fluorescence assays showed that RNA interference mediated by 3′ end biotinylated siRNA was

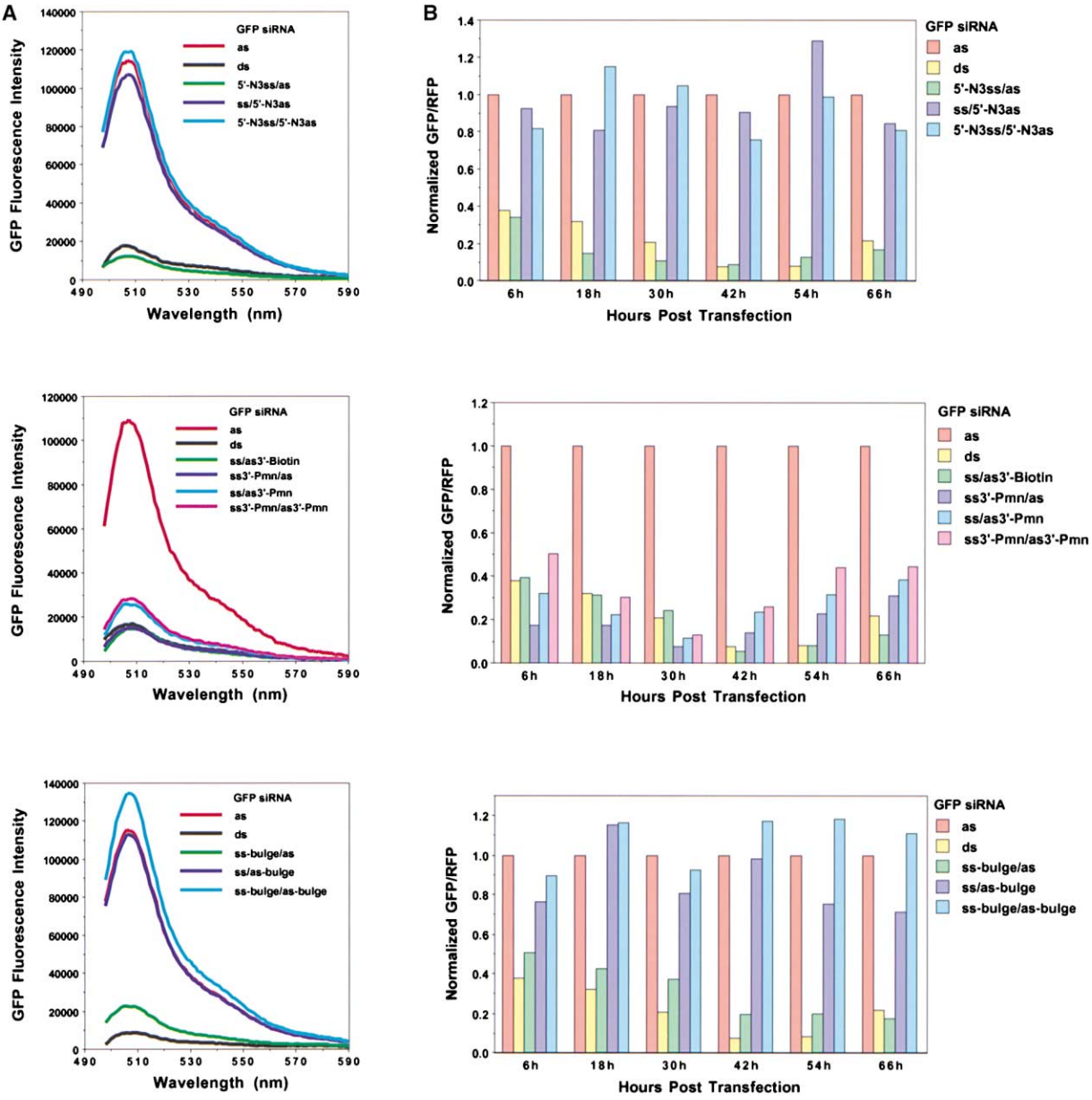

Figure 4. Quantitative Analysis of RNAi Effects in HeLa Cells Transfected with Modified siRNAs

pEGFP-C1 (as reporter), pDsRed1-N1 (as control) plasmids and 50 nM siRNA were cotransfected into HeLa cells by lipofectamine. Cells were harvested at various times after transfection. Fluorescence emission spectra of GFP and RFP in total cell lysates were detected by exciting at 488 and 568 nm, respectively.

(A) GFP emission spectra of modified siRNA-treated cells. Emission spectra of GFP in lysates from cells transfected with 5′-modified GFP siRNAs (upper panel), 3′-modified GFP siRNAs (middle panel), and bulge-containing GFP siRNAs (lower panel). For comparison, results from antisense- (as, red line) and unmodified duplex siRNA- (ds, black line) treated cells are included in each panel.

(B) Ratios of normalized GFP to RFP fluorescence intensity in lysates from modified siRNA-treated HeLa cells over 66 hr. The fluorescence intensity ratio of target (GFP) to control (RFP) fluorophore was determined in the presence of 5′-modified GFP siRNAs (upper panel), 3′-modified GFP siRNAs (middle panel), and bulge-containing GFP siRNAs (lower panel) and normalized to the ratio observed in the presence of antisense strand siRNA. Normalized ratios less than 1.0 indicate specific RNA interference effects. For comparison, results from antisense RNA and duplex siRNA-treated cells are included in each panel (as, orange bars; ds, yellow bars).

as effective as unmodified siRNA (Figures 3f and 3b; Figures 4A and 4B, middle panel). RNA interference is seen as early as 6 hr post-siRNA transfection and can be maintained for 42 hr posttransfection. Our ability to isolate biotin-RNA from cells after RNA interference had been initiated indicates that biotin was not removed from the RNA and rules out the possibility of siRNA 3′ OH termini involvement in the RNA interference pathway in human cells.

Second, in this biotin pull-out assay, only siRNA with 5′ OH ends can be ^{32}P-labeled by T4 PNK. As shown in Figure 5, the siRNA without SAP treatment was not

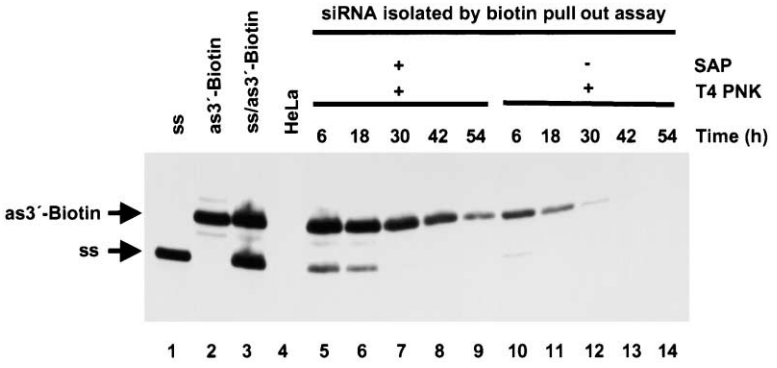

Figure 5. Isolation of 5′ End Phosphorylated and 3′ End Biotinylated siRNA from HeLa Cells

HeLa cells were cotransfected with biotinylated GFP duplex siRNA (ss/as3′-Biotin) and pEGFP-C1 plasmid as described in the Experimental Procedures. The siRNA was isolated by pull-out assay and subjected to phosphatase and kinase reactions (see Experimental Procedures). In brief, streptavidin magnetic beads were used to pull out biotinylated siRNAs from transfected cells, washed to remove unbound RNA, and split into two aliquots. One aliquot was dephosphorylated with shrimp alkaline phosphatase (SAP), and the RNA 5′ ends were labeled with ^{32}P by T4 polynucleotide kinase (PNK) reaction. The other aliquot was not dephosphorylated. RNA was resolved on 20% polyacrylamide-7 M Urea gels and visualized by phosphorimager analysis. Lanes 1–3 (marker lanes) contain 5′ end-labeled RNA: lane 1, sense strand (ss); lane 2, 3′ biotinylated antisense strand (as3′-Biotin); lane 3, heat denatured (10 min at 95°C) siRNA duplex (ss/as3′-Biotin). Lanes 5–14, isolated biotinylated siRNA with SAP treatment (lanes 5–9) or without (lanes 10–14). Lane 4, RNA isolated as above from HeLa cells without siRNA transfection.

efficiently labeled by T4 PNK (e.g., compare lane 10 to lane 5 and lane 11 to lane 6), indicating that the 5′ termini of siRNA did not contain free OH groups in vivo. These 5′ terminal groups can be removed by alkaline phosphatase treatment for subsequent radiolabeling (Figure 5, lanes 5–9), indicating that the 5′ termini of the siRNA had been phosphorylated in vivo.

Third, only the antisense strand is recovered by biotin pull-out assays. siRNA duplexes were 5′ end labeled with ^{32}P by T4 PNK, heat denatured (10 min at 95°C), and analyzed on a polyacrylamide-7 M urea denaturing gel. As shown in Figure 5 (lane 3), two single-stranded RNA species corresponding to the sense and biotinylated-antisense strands were observed, indicating that the siRNA duplexes were fully denatured under these conditions. Denatured siRNA duplexes contained approximately equal molar amounts of the sense and the antisense strands of RNA (Figure 5, lane 3). The cells were transfected with duplex siRNA, but the major products of the isolated siRNA (Figure 5, lanes 5–9) by biotin pull-out assay exhibited electrophoretic moblities identical to the antisense strand (lane 3), indicating that only biotinylated antisense strands were being recovered. These results suggest that RISC melts the duplex siRNA and separates the antisense from the sense strand during RNA interference in vivo.

Complete Unwinding of siRNA Duplex Is Not Necessary for RNA Interference Pathway In Vivo

ATP-dependent unwinding of the siRNA duplex in the RISC has been proposed to activate the complex to generate RISC*, which is competent to mediate RNAi (Nykanen et al., 2001). Although unwinding of siRNA in *Drosophila* embryo lysates has been demonstrated in the presence of ATP, the efficiency of unwinding seems low since only 5% of unwound siRNA was detected (Nykanen et al., 2001).

To examine whether or not the siRNA duplex in human cells is completely unwound, we performed RNA interference experiments with siRNA duplexes covalently crosslinked by psoralen photochemistry. Psoralens are bifunctional furocoumarins that intercalate between the base pairs of double-stranded nucleic acids and can photoreact with pyrimidine bases to form monoadducts and crosslinks (for review see Cimino et al., 1985). The structure of the psoralen derivative, 4′-(hydroxymethyl)-4,5′,8-trimethylpsoralen (HMT) used in this study is shown in Figure 6A. Psoralen crosslinking involves two successive photochemical reactions that take place at the 3,4 or 4′,5′ double bonds of psoralen (Cimino et al., 1985). Upon long-wave UV irradiation (320–400 nm), the intercalated psoralen can photoreact with adjacent pyrimidine bases to form either furan-side or pyrone-side monoadducts, which are linked to only one strand of the helix (Cimino et al., 1985). By absorbing a second photon, the furan-side monoadducts can be driven into diadducts, which are covalently linked to both strands of the helix (Hearst et al., 1984; Kanne et al., 1982). Psoralen crosslink formation occurs only when psoralen adds to adjacent and opposite pyrimidine bases in the double helix. The reaction is primarily with uracil in native RNAs, but reactions with cytidine have also been reported (Lipson et al., 1988; Thompson and Hearst, 1983; Turner and Noller, 1983). Based on psoralen photoreactivity, three possible psoralen crosslink sites in the GFP siRNA duplex are shown in Figure 6B. Note that there is no chance for all three sites to be crosslinked in one RNA.

Unlike the noncrosslinked ds siRNA, the two strands of the crosslinked siRNA duplex could not separate from each other under denaturing conditions so that the crosslinked siRNA duplex showed characteristically retarded mobility in polyacryalmide gel electrophoresis (PAGE) containing 7 M urea (Figure 6C). Crosslinking efficiency depended on the psoralen concentration (Figure 6C, lanes 2 and 3). To further verify the presence of crosslinks in the RNA helix and rule out the possibility of only monoadduct formation, the psoralen crosslinks were irradiated with short wave UV (254 nm), which showed photoreversal of the crosslinked bonds (Figure 6C, lane 4). The crosslinked siRNA duplex (Figure 6C, lane 3, upper band) was excised from the gel and purified. As control, the noncrosslinked siRNA that was irradiated with long wave UV (360 nm) (Figure 6C, lane 3, lower band) was also purified by the same method. The structures of the purified noncrosslinked and psoralen crosslinked siRNA duplexes were confirmed by PAGE

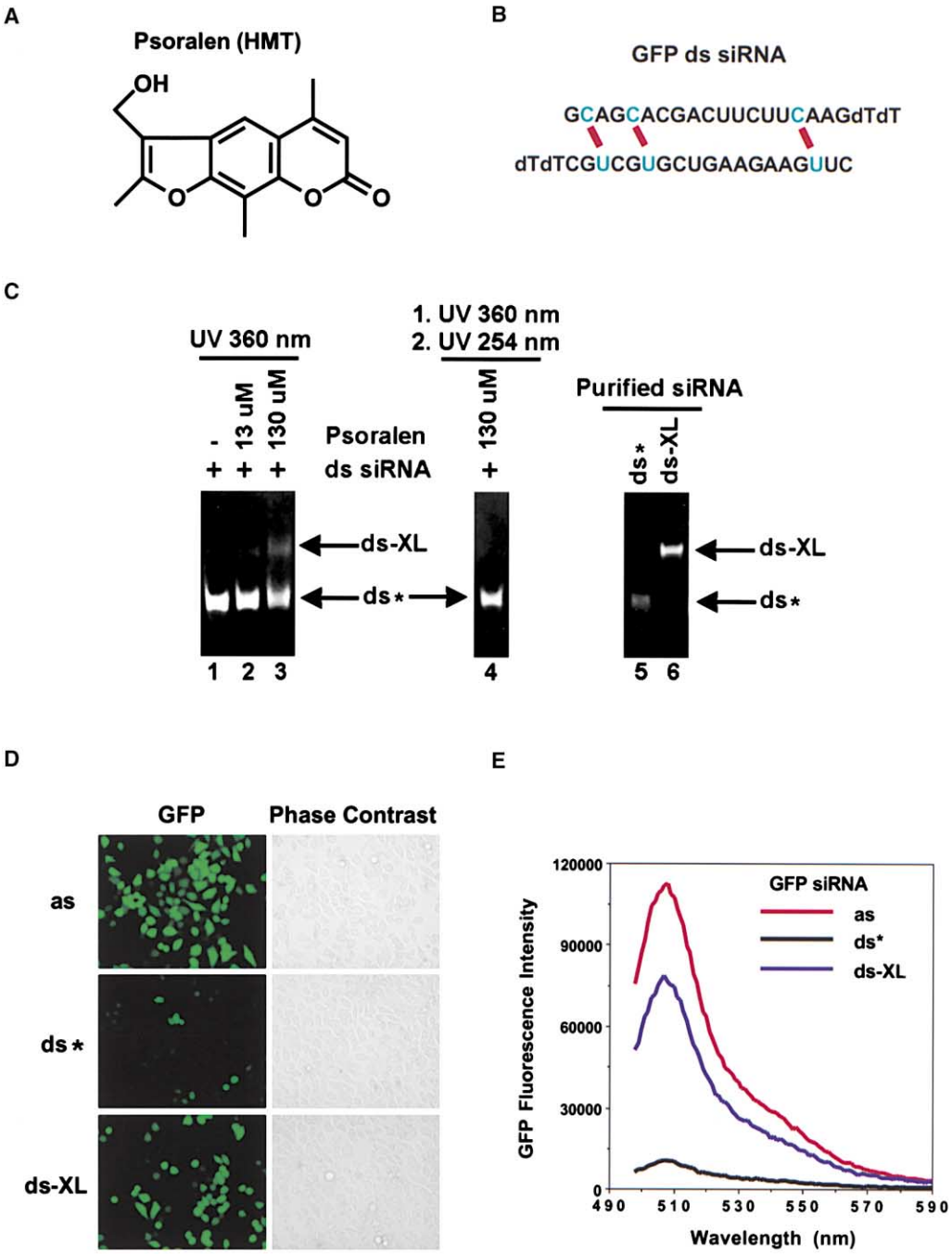

Figure 6. RNA Interference Activities of Covalently Photocrosslinked Duplex RNA in HeLa Cells

(A) Structure of a psoralen derivative, 4′-hydroxymethyl-4,5′,8-trimethylpsoralen (HMT), used to crosslink the duplex RNA.

(B) Photocrosslinking sites in GFP siRNA. Three preferred sites for psoralen addition to a duplex RNA are shown by cyan letters with red bars indicating the C-U crosslinks formed by UV irradiation in the presence of HMT.

(C) Psoralen photocrosslinking of siRNA duplexes. Mixtures of siRNA duplex and psoralen were exposed to UV 360 nm and denatured. Crosslinked and noncrosslinked siRNAs were resolved on 20% PAGE containing 7 M urea (lanes 2 and 3). UV-irradiated RNA bands were excised from the gel and purified. Purified crosslinked dsRNA (ds-XL) and noncrosslinked dsRNA (ds*) are shown in lanes 6 and 5, respectively. To confirm the nature and purity of the crosslink, a portion of the 360 nm UV-irradiated sample (lane 3) was UV irradiated at 254 nm. Photoreversal of psoralen crosslinked siRNA resulted in products with similar electrophoretic mobility to the siRNA duplex without HMT treatment (lane 4).

(D) Fluorescence images showing RNA interference effects of psoralen photocrosslinked siRNAs in living HeLa cells. Purified crosslinked ds siRNA (ds-XL, bottom panels) was cotransfected with reporter pEGFP-C1 and control pDsRed1-N1 plasmids into HeLa cells for dual fluorescence reporter assays. Fluorescence (left panels) and phase contrast (right panels) images of living cells were taken 48 hr posttransfection. For comparison, images from noncrosslinked ds siRNA (ds*, middle panels) and antisense siRNA (as, top panels) are also shown.

(E) GFP emission spectra of psoralen photocrosslinked siRNA duplex-treated cells. Cell lysates were prepared from HeLa cells treated with antisense siRNA (as), unmodified UV-irradiated duplex siRNA (ds*), and crosslinked ds siRNA (ds-XL) and analyzed by fluorescence spectroscopy. Fluorescence emission spectra of GFP and RFP were detected by exciting at 488 and 568 nm, respectively. GFP emission spectra are shown normalized to RFP expression.

containing 7 M urea (Figure 6C, lanes 5 and 6). Fluorescence imaging of living cells treated with crosslinked siRNA duplex showed that the siRNA duplex's inability to separate on PAGE did not completely abolish its RNA interference activity (Figure 6D, ds-XL). Quantitative analysis of GFP fluorescence intensity indicated that crosslinked siRNA retained 30% of its RNAi activity (Figure 6E, blue line). These results demonstrate that a complete unwinding of the siRNA duplex is not required for gene silencing in vivo (see Discussion).

There is a possibility that the psoralen crosslink of RNA can be photoreversed during transfection, repaired or removed by some unknown mechanism inside the cells, which might cause the partial RNA interference effect in vivo observed in Figures 6D and 6E. To rule out this possibility, we carried out a psoralen crosslinking experiment with siRNA duplex containing biotin at the 3′ end of the antisense strand. The crosslinked duplex (ss/as3′-Biotin-XL) was isolated and purified as described above and transfected into HeLa cells by lipofectamine. Biotinylated siRNA was isolated from the cells 30 hr posttransfection by biotin pull-out assay, SAP treated, and ^{32}P-labeled by T4 PNK as described above. The biotinylated siRNA was still crosslinked (Figure 7, lane 7) at 30 hr posttransfection. When UV irradiated (254 nm), this higher molecular weight siRNA species was converted into two RNA species corresponding to sense and antisense strands (Figure 7, lane 8), indicating the reversibility of the psoralen crosslink. These results show that crosslinked siRNA duplexes can enter the RNAi pathway.

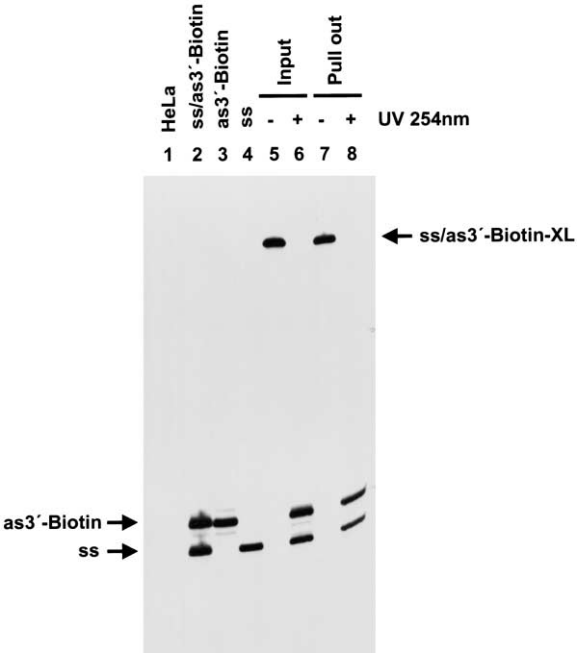

Figure 7. Isolation of Psoralen-Crosslinked siRNA from Human Cells

siRNA duplexes were conjugated with 3′ biotin (ss/as3′-Biotin), psoralen crosslinked, and purified as described in Figure 6 and in the Experimental Procedures. HeLa cells were cotransfected by lipofectamine with crosslinked siRNA (ss/as3′-Biotin-XL) and pEGFP-C1 plasmid, and siRNAs were isolated by biotin pull-out assay at 30 hr posttransfection as described in the Experimental Procedures. In brief, streptavidin-magnetic beads with biotinylated siRNA were subjected to phosphatase treatment and 5′ end labeled with ^{32}P. RNA was resolved on 20% polyacrylamide-7 M urea gels and visualized by phosphorimager analysis. Lane 1, RNA from HeLa cells without siRNA transfection. Lane 2, ^{32}P-labeled noncrosslinked siRNA duplex (ss/as3′-Biotin). Lane 3, ^{32}P-labeled 3′ biotinylated antisense strand siRNA (as3′-Biotin). Lane 4, ^{32}P-labeled sense strand RNA (ss). Lane 5, ^{32}P-labeled crosslinked siRNA duplex (ss/as3′-Biotin-XL). Lanes 7 and 8, siRNA isolated from HeLa cells treated with crosslinked siRNA duplex (ss/as3′-Biotin-XL). Lanes 6 and 8, UV irradiation (254 nm) of crosslinked siRNA to photoreverse the psoralen crosslinks.

Discussion

By using a quantitative dual fluorescence-based system, we have dissected the kinetics and a number of important parameters involved in the RNAi pathway in cultured human cells. Our results highlight the role of free 5′ end hydroxyl groups and the requirement of an A-form helical structure between the antisense strand and the target mRNA. We also found that a complete unwinding of the siRNA helix is not necessary to cause RNAi effects in vivo.

The time-dependent effect of siRNA may reflect a time lag between target mRNA degradation and the half-life of the existing protein expressed from the target gene. This time dependence may also indicate that the siRNAs need to be processed or assembled into an active complex with cellular factors for effective RNA interference.

Although RNA interference lasted at least 66 hr in HeLa cells, quantitative analysis indicated that inhibition by siRNAs did not persist. After reaching maximal activity at 42 hr posttransfection, RNA interference started to decrease at 54 hr, with only 70% inhibition activity at 66 hr. We also found that 5%–10% protein expressed from the genes targeted by siRNA remained at 42 hr posttransfection, but protein amount showed gradual recovery to normal levels between 66 to 90 hr (3 to 4 days) posttransfection (Y.-L.C. and T.M.R., unpublished data). The recovery of target gene expression also indicates that RNA interference by exogenous siRNA duplex does not exist forever in mammalian cells. These findings suggest that the proposed amplification system driven by RdRP and present in plants and nematodes may not exist or has very little effect on siRNA-mediated gene silencing in mammalian cells.

Recent studies have shown that synthetic siRNAs containing 5′-OH termini can successfully induce RNAi effects in *Drosophila* embryo lysates (Elbashir et al., 2001c; Nykanen et al., 2001) and cultured mammalian cells (Elbashir et al., 2001a). A model involving a 5′ end kinase activity necessary for RNA interference has been proposed (Nykanen et al., 2001). To our knowledge, however, there is no evidence that the 5′ end hydroxyl is required for in vivo interference activity. Our results show that replacing the 5′ OH, a kinase target site, with amino groups inhibited RNAi activity. Further isolation of siRNA by biotin pull-out experiments revealed that prior phosphatase activity was required for in vitro 5′ end radiolabeling by a polynucleotide kinase. Taken together, these results provide strong evidence for the requirement of 5′ end kinase activity for RNA interference effects in vivo.

What about a free 3′ end for RNAi effects in vivo? An RNA-directed RNA polymerase (RdRP) chain reaction, primed by siRNA, has recently been proposed to amplify the interference effects of a small amount of trigger RNA (reviewed in Nishikura, 2001). Lipardi et al. (2001) have shown siRNA-primed RNA synthesis in *Drosophila* embryo lysates and suggested that RNAi in *Drosophila* involves an RdRP where siRNA primes the conversion of target RNA to dsRNA. Further evidence of RdRP involvement in the RNAi pathway in *C. elegans* has been provided in studies (Sijen et al., 2001) showing target RNA-templated synthesis of new dsRNA. These studies highlight the importance of a 3′ hydroxyl in priming subsequent RdRP reactions. An RdRP homolog has not yet been identified in the human genome, suggesting the presence of a separate enzyme that can carry out primer-dependent replication of an RNA template. Our results demonstrate that blocking the 3′ position did not significantly affect RNAi activity of siRNA in human cells. Results of our kinetic experiments show that the interference effect lasted only ~4 days, indicating the absence of an amplification mechanism in human cells. In addition, our biotin pull-out experiments show that the 3′ end biotin groups on the antisense strand were not efficiently removed during RNAi activities in HeLa cells. Based on these studies, we suggest a model where RNA amplification by RNA-dependent RNA polymerase is not essential for RNA interference in mammalian cell lines.

It is interesting to note that we found no requirement for a perfect A-form helix in siRNA for interference effects in HeLa cells, but an A-form structure was required for antisense-target RNA duplexes. These results suggest an RNAi mechanism where RISC formation does not involve perfect RNA helix recognition, but RISC* assembly requires an A-form helical structure.

The most intriguing results were obtained by crosslinking siRNAs and testing their interference activities in HeLa cells. Psoralen crosslinked siRNA duplexes retained 30% of RNA interference activity. This result can be explained by psoralen photocrosslinking chemistry. There are three possible sites in the GFP siRNA duplex where psoralen can crosslink, yet the crosslinking reaction is not efficient enough to create multiple crosslinks in a single given siRNA duplex (Cimino et al., 1985; Thompson and Hearst, 1983). Thus, in the purified crosslinked siRNA duplex population, about one-third had crosslinking at the site near the 5′ end of the antisense strand, about one-third had crosslinking in the middle region, and the rest had crosslinking near the 3′ end of the antisense strand.

We already showed that accessibility to the 5′ termini of the antisense strand is required for efficient RNA interference in vivo. 5′ phosphorylation of the antisense strand is also required for RNA interference in vitro (Nykanen et al., 2001). The cleavage site on target mRNA has been shown to be determined by the 5′ end position of the target-recognizing siRNA (Elbashir et al., 2001c). Based on these findings, we suggest that unwinding of the siRNA duplex would start from the 5′ end of the antisense strand, which sets the ruler for target mRNA cleavage. If crosslinking occurred near the 5′ end of the antisense strand, it would completely prohibit the unwinding of the siRNA duplex and block access to the 5′ termini of the antisense strand, which would completely abolish the RNAi effect. If crosslinking occurred in the middle of the siRNA duplex, near the cleavage site of mRNA, we suggest that, although the siRNA duplex could still undergo some unwinding, this crosslink might interfere with the pairing between target mRNA and the guiding siRNA, thus also blocking the RNAi effect. If crosslinking occurred near the 3′ end of the antisense strand, the duplex RNA could unwind, not completely but sufficient for the antisense strand to hybridize to the target mRNA. We have already shown that blocking either the 3′ end of the antisense strand or the 5′ end of the sense strand has no significant effect on its RNAi activity. It would thus be reasonable to believe that a siRNA duplex with crosslinking near the 3′ end of the antisense strand may still be competent in RNA interference. This hypothesis also explains the remaining 30% RNAi activity in the psoralen-crosslinked siRNA duplex.

These results suggest a possible model for the RNAi pathway in human cells. An RNA-protein complex containing siRNA (RISC) is assembled without the requirement for an A-form RNA helix and/or a free 3′-OH. The 5′-OH of the siRNA duplex is phophorylated by a kinase. During activation of RISC to RISC*, a 5′→3′ helicase unwinds the RNA duplex to allow hybridization between the antisense strand of siRNA and the target RNA. The requirement of a perfect A-form helix at this stage strongly suggests that another protein (or protein complex) binds this RNA duplex, either in a structural role and/or assisting in the cleavage of mRNA. A complete unwinding of the siRNA duplex is not required for this process, nor can this interference activity be amplified via the 3′ end. However, unwinding of the duplex up to the cleavage site may be necessary so that the antisense strand can form an A-form helix with the target strand for further protein interactions. These results also argue against the involvement of RNA amplification mechanism(s) for RNA interference in human cells.

In summary, our results provide new insight into the mechanism of RNAi in mammalian cells, and these results could guide the design of siRNA structures useful in probing biological questions and in functional genomic studies.

Experimental Procedures

siRNA Preparation

Twenty-one nucleotide RNAs were chemically synthesized as 2′ bis(acetoxyethoxy)-methyl ether-protected oligos by Dharmacon (Lafayette, CO). Synthetic oligonucleotides were deprotected, annealed, and purified as described by the manufacturer. Successful duplex formation was confirmed by 20% nondenaturing polyacrylamide gel electrophoresis (PAGE). All siRNAs were stored in DEPC (0.1% diethyl pyrocarbonate)-treated water at −80°C. The sequences of GFP or RFP target-specific siRNA duplexes were designed according to the manufacturer's recommendation and subjected to a BLAST search against the human genome sequence to ensure that no endogenous genes of the genome were targeted.

Culture and Transfection of Cells

HeLa cells were maintained at 37°C in Dulbecco's modified Eagle's medium (DMEM, Invitrogen) supplemented with 10% fetal bovine serum (FBS), 100 units/ml penicillin, and 100 μg/ml streptomycin (Invitrogen). Cells were regularly passaged at subconfluence and plated 16 hr before transfection at 70% confluency. Lipofectamine (Invitrogen)-mediated transient cotransfections of reporter plasmids

and siRNAs were performed in duplicate 6-well plates as described by the manufacturer for adherent cell lines. A transfection mixture containing 0.66 μg pEGFP-C1 and 1.33 μg pDsRed1-N1 reporter plasmids (Clontech), 50 nM siRNA, and 10 μl lipofectamine in 1 ml serum-reduced OPTI-MEM (Invitrogen) was added to each well. Cells were incubated in transfection mixture for 6 hr and further cultured in antibiotic-free DMEM. Cells were treated under the same conditions without siRNA for mock experiments. At various time intervals, the transfected cells were washed twice with phosphate-buffered saline (PBS, Invitrogen), flash frozen in liquid nitrogen, and stored at −80°C for reporter gene assays.

In Vivo Fluorescence Analysis

pEGFP-C1, pDsRed1-N1 reporter plasmids and 50 nM siRNA were cotransfected into HeLa cells by lipofectamine as described above except that cells were cultured on 35 mm plates with glass bottoms (MatTek Corporation, Ashland, MA) instead of standard 6-well plates. Fluorescence in living cells was visualized 48 hr posttransfection by conventional fluorescence microscopy (Zeiss). For GFP and RFP fluorescence detection, FITC and CY3 filters were used, respectively.

Dual Fluorescence Reporter Gene Assays

pEGFP-C1, pDsRed1-N1 reporter plasmids and 50 nM siRNA were cotransfected into HeLa cells. EGFP-C1 encoded enhanced green fluorescence protein (GFP), while DsRed1-N1 encoded red fluorescence protein (RFP). Cells were harvested as described above and lysed in ice-cold reporter lysis buffer (Promega) containing protease inhibitor (complete, EDTA-free, 1 tablet/10 ml buffer, Roche Molecular Biochemicals). After clearing the resulting lysates by centrifugation, protein in the clear lysate was quantified by Dc protein assay kit (Bio-Rad). One hundred twenty micrograms of total cell lysate in 160 μl reporter lysis buffer was measured by fluorescence spectroscopy (Photon Technology International). The slit widths were set at 4 nm for both excitation and emission. All experiments were carried out at room temperature. Fluorescence of GFP in cell lysates was detected by exciting at 488 nm and recording from 498–650 nm. The spectrum peak at 507 nm represents the fluorescence intensity of GFP. Fluorescence of RFP in the same cell lysates was detected by exciting at 568 nm and recording from 588–650 nm; the spectrum peak at 583 nm represents the fluorescence intensity of RFP. The fluorescence intensity ratio of target (GFP) to control (RFP) fluorophore was determined in the presence of siRNA duplex and normalized to that observed in the presence of antisense strand siRNA. Normalized ratios less than 1.0 indicate specific interference.

Western Blotting

Cell lysates were prepared from siRNA-treated cells and analyzed as described above. Proteins in 30 μg of total cell lysate were resolved by 10% SDS-PAGE, transferred onto a polyvinylidene difluoride membrane (PVDF membrane, Bio-Rad), and immunoblotted with antibodies against EGFP and DsRed1-N1 (Clontech). For loading control, the same membrane was also blotted with anti-actin actibody (Santa Cruz). Protein content was visualized with a BM Chemiluminescence Blotting Kit (Roche Molecular Biochemicals). The blots were exposed to X-ray film (Kodak MR-1) for various times (between 30 s and 5 min).

Psoralen Photocrosslink of siRNA Duplex

Forty micrograms of siRNA duplex was incubated with 132 μM of a psoralen derivative, 4′-hydroxymethyl-4,5′,8-trimethylpsoralen (HMT) in 200 μl DEPC-treated water at 30°C for 30 min. Mixtures of siRNA duplex and HMT were exposed to UV 360 nm at 4°C for 20 min, then denatured by mixing with 400 μl formamide/formaldehyde (12.5:4.5) RNA loading buffer and heating at 95°C for 15 min. Crosslinked siRNA duplex and noncrosslinked siRNA were resolved by 20% PAGE containing 7 M urea in Tris-borate-EDTA. Crosslinked siRNA duplexes appeared as a population with retarded electrophoretic mobility compared to the noncrosslinked species. RNAs were cut from the gel and purified by C18 reverse-phase column chromatography (Waters). Purified crosslinked dsRNA and noncrosslinked dsRNA were used in dual fluorescence reporter assays as described above, except that all procedures were performed in the dark to avoid light effects on psoralen. To ensure that the crosslink depended on the presence of psoralen, part of the UV 360 nm treated mixture was also subjected to UV 254 nm at 4°C for 20 min. Photoreverse-crosslinked siRNA migrated in 20% polyacrylamide-7 M urea gels with similar mobility to the siRNA duplex without HMT treatment.

Biotin Pull-Out Assay for siRNA Isolation from Human Cells

Antisense strands of the siRNA duplex were chemically synthesized and biotin-conjugated at the 3′ end (Dharmacon, Lafayette, CO). Synthetic oligonucleotides were deprotected and annealed with the unmodified sense strand RNA to form duplex siRNA (ss/as3′-Biotin). HeLa cells, which had been plated at 70% confluency in 100 mm dishes, were cotransfected with duplex siRNA (~600 pmole) and EGFP-C1 plasmid (1 μg) by a lipofectamine-mediated method as described above. At various times, the transfected cells were washed twice with PBS (Invitrogen) and flash frozen in liquid nitrogen. Low molecular weight RNA was isolated from the cells using a Qiagen RNA/DNA Mini Kit. Biotinylated siRNA was pulled out by incubating purified RNA with streptavidin-magnetic beads (60 μl) in TE buffer (10 mM Tris-HCl [pH 8.0], 1 mM EDTA) containing 1 M NaCl at room temperature for 3 hr. The beads were washed four times with 200 μl TE buffer, resuspended in 100 μl TE buffer, and split into two equal aliquots. To one aliquot (50 μl), we added 50 units of shrimp alkaline phosphatase (SAP, Roche Molecular Biochemicals) in 1× SAP buffer and incubated at 37°C for 1 hr. The SAP reaction was then stopped by heating at 65°C for 15 min and washed four times with 200 μl TE buffer. The other aliquot was not treated with SAP. Aliquots of beads with or without SAP treatment were incubated with 30 units T4 polynucleotide kinase (T4 PNK, Roche Molecular Biochemicals) in 30 μl 1× PNK buffer containing 0.2 mCi γ-^{32}P ATP at 37°C for 1 hr. RNA products were resolved on 20% polyacrylamide-7 M urea gels and ^{32}P-labeled RNAs were detected by phosphorimaging.

Acknowledgments

This work was supported by NIH grants AI43198, AI41404, and AI45466.

Received: May 30, 2002
Revised: September 6, 2002

References

Bass, B.L. (2000). Double-stranded RNA as a template for gene silencing. Cell *101*, 235–238.

Bernstein, E., Caudy, A.A., Hammond, S.M., and Hannon, G.J. (2001). Role for a bidentate ribonuclease in the initiation step of RNA interference. Nature *409*, 363–366.

Cimino, G.D., Gamper, H.B., Isaacs, S.T., and Hearst, J.E. (1985). Psoralens as photoactive probes of nucleic acid structure and function: organic chemistry, photochemistry, and biochemistry. Annu. Rev. Biochem. *54*, 1151–1193.

Cogoni, C., and Macino, G. (1999). Gene silencing in *Neurospora crassa* requires a protein homologous to RNA-dependent RNA polymerase. Nature *399*, 166–169.

Cogoni, C., and Macino, G. (2000). Post-transcriptional gene silencing across kingdoms. Curr. Opin. Genet. Dev. *10*, 638–643.

Dalmay, T., Hamilton, A., Rudd, S., Angell, S., and Baulcombe, D.C. (2000). An RNA-dependent RNA polymerase gene in *Arabidopsis* is required for posttranscriptional gene silencing mediated by a transgene but not by a virus. Cell *101*, 543–553.

Elbashir, S.M., Harborth, J., Lendeckel, W., Yalcin, A., Weber, K., and Tuschl, T. (2001a). Duplexes of 21-nucleotide RNAs mediate RNA interference in cultured mammalian cells. Nature *411*, 494–498.

Elbashir, S.M., Lendeckel, W., and Tuschl, T. (2001b). RNA interference is mediated by 21- and 22-nucleotide RNAs. Genes Dev. *15*, 188–200.

Elbashir, S.M., Martinez, J., Patkaniowska, A., Lendeckel, W., and Tuschl, T. (2001c). Functional anatomy of siRNAs for mediating effi-

cient RNAi in *Drosophila melanogaster* embryo lysate. EMBO J. *20*, 6877–6888.

Fire, A., Xu, S., Montgomery, M.K., Kostas, S.A., Driver, S.E., and Mello, C.C. (1998). Potent and specific genetic interference by double-stranded RNA in *Caenorhabditis elegans*. Nature *391*, 806–811.

Grishok, A., Tabara, H., and Mello, C.C. (2000). Genetic requirements for inheritance of RNAi in *C. elegans*. Science *287*, 2494–2497.

Hamilton, A.J., and Baulcombe, D.C. (1999). A species of small antisense RNA in posttranscriptional gene silencing in plants. Science *286*, 950–952.

Hammond, S.M., Bernstein, E., Beach, D., and Hannon, G.J. (2000). An RNA-directed nuclease mediates post-transcriptional gene silencing in *Drosophila* cells. Nature *404*, 293–296.

Hammond, S.M., Caudy, A.A., and Hannon, G.J. (2001). Post-transcriptional gene silencing by double-stranded RNA. Nat. Rev. Genet. *2*, 110–119.

Hearst, J.E., Isaacs, S.T., Kanne, D., Rapoport, H., and Straub, K. (1984). The reaction of the psoralens with deoxyribonucleic acid. Q. Rev. Biophys. *17*, 1–44.

Kanne, D., Straub, K., Rapoport, H., and Hearst, J.E. (1982). Psoralen-deoxyribonucleic acid photoreaction. Characterization of the monoaddition products from 8-methoxypsoralen and 4,5′8-trimethylpsoralen. Biochemistry *21*, 861–871.

Kennerdell, J.R., and Carthew, R.W. (1998). Use of dsRNA-mediated genetic interference to demonstrate that frizzled and frizzled 2 act in the wingless pathway. Cell *95*, 1017–1026.

Ketting, R.F., and Plasterk, R.H. (2000). A genetic link between cosuppression and RNA interference in *C. elegans*. Nature *404*, 296–298.

Lipardi, C., Wei, Q., and Paterson, B.M. (2001). RNAi as random degradative PCR: siRNA primers convert mRNA into dsRNAs that are degraded to generate new siRNAs. Cell *107*, 297–307.

Lipson, S.E., Cimino, G.D., and Hearst, J.E. (1988). Structure of M1 RNA as determined by psoralen cross-linking. Biochemistry *27*, 570–575.

Matzke, M., Matzke, A.J., and Kooter, J.M. (2001). RNA: guiding gene silencing. Science *293*, 1080–1083.

Mourrain, P., Beclin, C., Elmayan, T., Feuerbach, F., Godon, C., Morel, J.B., Jouette, D., Lacombe, A.M., Nikic, S., Picault, N., et al. (2000). *Arabidopsis SGS2* and *SGS3* genes are required for posttranscriptional gene silencing and natural virus resistance. Cell *101*, 533–542.

Neenhold, H.R., and Rana, T.M. (1995). Major groove opening at the HIV-1 Tat binding site of TAR RNA evidenced by a rhodium probe. Biochemistry *34*, 6303–6309.

Nishikura, K. (2001). A short primer on RNAi: RNA-directed RNA polymerase acts as a key catalyst. Cell *107*, 415–418.

Nykanen, A., Haley, B., and Zamore, P.D. (2001). ATP requirements and small interfering RNA structure in the RNA interference pathway. Cell *107*, 309–321.

Parrish, S., Fleenor, J., Xu, S., Mello, C., and Fire, A. (2000). Functional anatomy of a dsRNA trigger: differential requirement for the two trigger strands in RNA interference. Mol. Cell *6*, 1077–1087.

Sharp, P.A. (2001). RNA interference—2001. Genes Dev. *15*, 485–490.

Sijen, T., and Kooter, J.M. (2000). Post-transcriptional gene-silencing: RNAs on the attack or on the defense? Bioessays *22*, 520–531.

Sijen, T., Fleenor, J., Simmer, F., Thijssen, K.L., Parrish, S., Timmons, L., Plasterk, R.H., and Fire, A. (2001). On the role of RNA amplification in dsRNA-triggered gene silencing. Cell *107*, 465–476.

Smardon, A., Spoerke, J.M., Stacey, S.C., Klein, M.E., Mackin, N., and Maine, E.M. (2000). EGO-1 is related to RNA-directed RNA polymerase and functions in germ-line development and RNA interference in *C. elegans*. Curr. Biol. *10*, 169–178.

Stark, G.R., Kerr, I.M., Williams, B.R., Silverman, R.H., and Schreiber, R.D. (1998). How cells respond to interferons. Annu. Rev. Biochem. *67*, 227–264.

Thompson, J.F., and Hearst, J.E. (1983). Structure of *E. coli* 16S RNA elucidated by psoralen crosslinking. Cell *32*, 1355–1365.

Turner, S., and Noller, H.F. (1983). Identification of sites of 4′-(hydroxymethyl)-4,5′,8-trimethoxylpsoralen cross-linking in *Escherichia coli* 23S ribosomal ribonucleic acid. Biochemistry *22*, 4159–4164.

Tuschl, T. (2001). RNA interference and small interfering RNAs. Chembiochem *2*, 239–245.

Tuschl, T., Zamore, P.D., Lehmann, R., Bartel, D.P., and Sharp, P.A. (1999). Targeted mRNA degradation by double-stranded RNA in vitro. Genes Dev. *13*, 3191–3197.

Waterhouse, P.M., Wang, M.B., and Finnegan, E.J. (2001). Role of short RNAs in gene silencing. Trends Plant Sci. *6*, 297–301.

Weeks, K.M., and Crothers, D.M. (1991). RNA recognition by Tat-derived peptides: interaction in the major groove? Cell *66*, 577–588.

Weeks, K.M., and Crothers, D.M. (1993). Major groove accessibility of RNA. Science *261*, 1574–1577.

Yang, D., Lu, H., and Erickson, J.W. (2000). Evidence that processed small dsRNAs may mediate sequence-specific mRNA degradation during RNAi in *Drosophila* embryos. Curr. Biol. *10*, 1191–1200.

Zamore, P.D., Tuschl, T., Sharp, P.A., and Bartel, D.P. (2000). RNAi: double-stranded RNA directs the ATP-dependent cleavage of mRNA at 21 to 23 nucleotide intervals. Cell *101*, 25–33.